PAPER

NJC
www.rsc.org/njc

Laser pyrolysis studies of β-diketonate chemical vapour deposition precursors. Part 1: β-diketones

Douglas K. Russell* **and Anna Yee**

Department of Chemistry, University of Auckland, Private Bag 92019, Auckland, New Zealand.
E-mail: d.russell@auckland.ac.nz; Fax: +64 9 373 7422; Tel: +64 9 373 7599, ext: 88303

Received (in Montpellier, France) 9th August 2004, Accepted 21st September 2004
First published as an Advance Article on the web 19th January 2005

The thermal decomposition of the β-diketones pentane-2,4-dione, 1,1,1,5,5,5-hexafluoropentane-2,4-dione, and 2,2,6,6-tetramethylheptane-3,5-dione has been studied using the technique of IR laser-powered homogeneous pyrolysis combined with the *ab initio* calculation of activation energies of possible reaction pathways. Pentane-2,4-dione decomposes by two parallel molecular elimination pathways, the keto tautomer affording acetone and ketene *via* a 6-electron retroene reaction and the enol tautomer 2-methylfuran *via* H_2O elimination, followed by cyclisation. 1,1,1,5,5,5-Hexafluoropentane-2,4-dione eliminates HF with ring closure to yield 2,2-difluoro-5-(trifluoromethyl)furan-3(2*H*)-one. There is also a minor route of loss of one or two CF_3 radicals, followed by H-abstraction to yield 3,3-difluoroacryloylfluoride and carbon suboxide, respectively. 2,2,6,6-Tetramethylheptane-3,5-dione decomposes *via* central C–CO bond homolysis, followed by CO or ketene loss from the resultant radicals and subsequent disproportionation of *t*-Bu radicals to produce 2-methylpropene and 2-methylpropane.

Introduction

Transition metal complexes of the anions of β-diketone ligands such as acetylacetone (acacH, pentane-2,4-dione, **1**) have been well-known for many years and exhibit a range of structural motifs, reactivity and stability.[1] More recently, neutral β-diketone complexes have been exploited as volatile precursors to the deposition of metals in materials as diverse as semiconductors and high temperature superconductors.[2] While there has been considerable work of a developmental or exploratory nature, rather little is known about the detailed mechanisms of thermal decomposition of such complexes. We have shown that the technique of infrared laser-powered homogeneous pyrolysis (IR LPHP)[3,4] is uniquely suited to the elucidation of thermal decomposition reaction mechanisms.[5,6] When allied with standard analytical methods and augmented by techniques for the detection and identification of short-lived reaction intermediates and *ab initio* evaluation of the feasibility of reaction routes, very detailed information may be obtained. The value of this multilateral approach has been demonstrated in systems as varied as precursors to chemical vapour deposition,[7–11] various cyclic systems[12,13] and small organic molecules.[14]

In the present work, we report IR LPHP studies of the three common diketones acacH, 1,1,1,5,5,5-hexafluoropentane-2,4-dione (hexafluoroacetylacetone, hfacH, **2**), and 2,2,6,6-tetramethylheptane-3,5-dione (thdH, **3**). Not only are complexes derived from these used widely as deposition precursors, but the compounds themselves exhibit a range of thermal decomposition behaviour, resulting from subtle changes in the balance of keto-enol equilibria and bond strengths. In future work, we shall report parallel studies of β-diketonate complexes of the metals used in the production of the high temperature superconductors, namely Cu, Ba and Y.[15]

Experimental methods

Chemicals

All diketones and other compounds used were of analytical grade quality and obtained commercially. These and SF_6 (BOC) were purified before use by repeated freeze-pump-thaw cycles. Materials were handled on a Pyrex vacuum line fitted with greaseless J. Youngs taps; before use, the line was preconditioned by exposure to the vapour under study and re-evacuation. Precursor and product identification and analysis (FT-IR spectroscopy and GC-MS) were accomplished using commercial instrumentation in conjunction with comparison with data from authentic samples.

Infrared laser-powered homogeneous pyrolysis

All static cell pyrolyses utilised the IR LPHP technique. Since this method has been described in detail elsewhere, only a brief description is given here.[3–6] Pyrolysis is performed in a cylindrical Pyrex cell (length 100 mm, diameter 38 mm) fitted with ZnSe windows. Although ZnSe is opaque to infrared radiation below 500 cm^{-1}, it has several distinct advantages over cheaper materials, such as NaCl. ZnSe is strong and thermally stable, and non-hygroscopic. Most significantly, ZnSe is highly transparent to the CO_2 laser radiation. The pyrolysis cell is filled with between one and two torr (1 torr = 133.3 Pa) of the vapour under study and approximately 10 torr of SF_6. The contents of the cell are then exposed to the output of a free running CW CO_2 laser operating at 10.6 μm. The laser power level (*i.e.*, temperature) is generally set to initiate decomposition of the target compound, with an exposure time sufficient to provide an analysable yield of products, typically a few percent of decomposition. As shown elsewhere,[3,6] SF_6 strongly absorbs the laser radiation, which is then rapidly converted to heat *via* efficient inter-molecular and intra-molecular relaxation. The low thermal conductivity of SF_6 ensures that a strongly non-uniform temperature profile is produced in which the centre of the cell may reach temperatures of the order of 1500 K while the cell wall remains at room temperature.[16] An effective mean temperature may be determined by measuring the rate of disappearance of a compound of known decomposition kinetics.

IR LPHP has a number of well-documented advantages. The first of these is that pyrolysis is initiated directly in the gas

DOI: 10.1039/b412486n

phase, thereby eliminating the complications frequently introduced by competing surface reaction. The second is that the primary products of pyrolysis are rapidly ejected into the cooler regions of the cell, inhibiting their further reaction. In favourable cases, these products may be accumulated for further investigation. One disadvantage of IR LPHP is that the temperature of the pyrolysis is neither well-defined nor easily determined; comparison with more conventional methods of pyrolysis is thus difficult.

Under favourable circumstances, further mechanistic information may be obtained by the judicious use of additives. In particular, the formation of new products or a change in product distribution on co-pyrolysis with a few torr of H_2 or (even more revealingly) D_2 is strong indirect evidence for the involvement of free radicals. This well-established method is based on the rapid reaction of many radicals with H_2: $R + H_2 \rightarrow RH + H$.[17–19] We have exploited this to demonstrate, for example, the role played by thienyl radicals in the decomposition of thiophene.[13]

Analytical methods

The FTIR spectra presented in this work were recorded using a Digilab FTS-60 Fourier transform spectrometer at a resolution of 1 cm^{-1} and averaged over 32 scans per spectrum. Win-IR software was used to acquire and process spectral data. The sample compartment of the spectrometer, which contained the pyrolysis cell, was purged with N_2 to reduce/eliminate contributions of CO_2 and water from the ambient atmosphere. All spectra were collected against a background spectrum of an evacuated pyrolysis cell. FTIR spectra were used primarily to characterise small gaseous products such as CO, methane or ketene, where resolved vibration-rotation structure permits unambiguous identification even from a single band; in such cases, comparison with authentic samples was used. The technique is less useful for larger molecules, in which similar vibrations often have almost identical bands, and it also lacks the sensitivity necessary for quantitative analysis.

GC-MS analysis of gas samples was conducted using a Hewlett Packard 6890 series gas chromatograph interfaced with a Hewlett Packard 5793 mass selective detector (MSD). Base pressure of the MSD was maintained at 1×10^{-5} torr by a turbomolecular pump backed by a rotary pump. Gas samples were extracted from the pyrolysis cell, *via* the septum port, with a Hamilton 2.5 ml gas-tight syringe fitted with a lockable valve. The contents of the cell were at relatively low pressure (12–15 torr); typically, therefore, 2.5 ml of the gas sample were extracted and, after the syringe valve was engaged, the sample was compressed to 0.25 ml to achieve a pressure close to atmospheric. An "HP5-MS" cross-linked phenyl methyl siloxane gum capillary column (i.d.: 0.25 mm, length: 29.2 m, film thickness: 0.25 μm) was employed as a multi-purpose column, while a "GS GasPro" column (i.d.: 0.32 μm, length: 30 m) was used for the detection and identification of low molecular weight species. Helium was used as the carrier gas in this GC-MS system.

Matrix isolation spectroscopy

Short-lived intermediates were detected using matrix isolation FTIR spectroscopy. A two-stage closed-cycle helium refrigerator was used for all matrix isolation experiments. The second stage (heat station) of the cryostat, with which a copper sample holder was in direct contact, was maintained at a temperature of between 15 and 20 K for the duration of the experiment. All matrices were collected at this temperature. The matrix isolation assembly was constructed so that any reactive species, generated through IR LPHP of an appropriate precursor, would rapidly co-deposit with the matrix material on the cold sample holder. Spectra of short-lived species were distinguishable from those of stable products by observing their disappearance on careful annealing to a higher temperature (dependent on stability).

In matrix isolation studies, the gaseous pyrolysis mixture flowed from a vacuum line to the cold head through a ZnSe-fronted reaction cell into which the laser radiation was directed. While moderately short-lived species reach the cold head, extremely reactive species react further and are not observed. Consequently, by employing a Pyrex tube of variable length between the reaction cell and cold stage, it is possible to change the flow time between generation and collection, and hence to discriminate to some extent between short-lived intermediate species based on lifetimes.

This IR LPHP matrix isolation apparatus could be modified so that product gas flow along the path between the reaction cell and cold stage was restricted by passing through a narrow aperture. The use of an aperture to restrict gas flow elevated the pressure of SF_6 attainable in the IR LPHP cell. At a given laser power, the effective temperature was therefore significantly higher than that attained when the restriction was not employed. This was reflected in the laser power required to initiate decomposition; relatively stable compounds, which decomposed when the gas flow was restricted, remained intact even at the highest laser power available when the gas flow was unrestricted. When used, this modification of the matrix isolation assembly therefore allowed IR LPHP of compounds that could not be decomposed without, but precluded the observation of very reactive species.

Calculation methods

The feasibility of a proposed pyrolysis scheme could be evaluated by determining the relative activation energies involved. For the most part, this involved calculating the activation barrier to molecular elimination routes such as dehydration or bond homolysis, the predominant decomposition routes, and comparing these values with that of an alternative system, whose actual pyrolysis temperature (*i.e.*, the laser power required to initiate decomposition) was known. It was found that theory agreed well with experiment; a system calculated to possess higher activation energy required a higher decomposition temperature. Of course, an initial step may be followed by further processes if the latter also possess sufficiently low activation energies. Observed end products may therefore reflect a complex series of reactions, each of which must be feasible under the prevailing conditions.

All theoretical calculations were executed using the PC Spartan '02 molecular orbital program.[20,21] PC Spartan '02 provides a full range of molecular mechanics and quantum chemical methods, and it was found that the density functional theory method at the B3LYP level with the 6-31G* basis set[22] provided sufficiently accurate results. The one exception was for systems containing strong hydrogen bonds (for example, the enol forms of the diketones), for which it was found to be necessary to include the diffuse functions of the 6-311+G** basis set. Relative values of the activation energies of various reaction pathways were considered to be of greater value in predicting mechanism than absolute values. As a benchmark, the activation energy for 1,2-elimination of H_2O from ethanol was calculated as 300 kJ mol^{-1} with the 6-31G* basis set and 282 kJ mol^{-1} with the 6-311+G** basis set, both very comparable with the experimentally determined value of 281 kJ mol^{-1}.[23]

Results

Acetylacetone (pentane-2,4-dione), acacH

Previous work. Like all β-diketones, acacH exists largely as the internally enol form (**1**) at room temperatures, with the fraction of the keto form (**4**) increasing as temperature is raised. Thus, at room temperature, acacH is 81% enol, while at 230 °C it is 60% enol.[24] This equilibrium is likely to be reflected in the decomposition chemistry.

The earliest investigation of acetylacetone pyrolysis was conducted by Hurd and Tallyn in 1925 with the primary objective of producing ketene.[25] Liquid acetylacetone was subjected to temperatures between 610 and 700 °C to obtain varying yields of ketene; the optimum yield of 16.7% was obtained at 635 °C. The accompanying product from the decomposition of acetylacetone was acetone. Charles *et al.*[26] subsequently pyrolysed liquid acetylacetone at temperatures lower than those used by Hurd and Tallyn. The main gaseous products found upon pyrolysis at 346 °C were acetic acid and acetone, whilst at 462 °C substantial amounts of CO_2, CO and CH_4 were also detected. The latter products resulted from pyrolysis of acetic acid or acetone rather than from acetylacetone directly.

Both these examples of acetylacetone pyrolysis were conducted using conventional "hot-walled" techniques (where surface reactions are possible). To date, only two homogeneous pyrolysis studies of acetylacetone have been reported. Choudhury and Lin reported a high temperature (1120–1660 K) study using shock waves.[27] In that work, acetylacetone was observed to undergo pyrolysis *via* two concurrent pathways: (1) elimination of H_2O to yield $CH_3C{\equiv}CCOCH_3$ and/or $CH_2{=}C{=}CHCOCH_3$ and (2) α-β dissociation to produce $CH_3CO^\bullet$ and $CH_3COCH_2^\bullet$ radicals.[28] More recently, Al-awadi and co-workers have investigated the kinetics of the elimination reaction in a number of pentane-2,4-dione derivatives, including acacH, and have concluded that a concerted 6-membered elimination process is responsible for the production of acetone and ketene, rather than the radical pathway.[29,30]

Experimental results. In our work, IR LPHP of acetylacetone (acacH) was effected at a laser power of approximately 5 W, resulting in approximately 10% decomposition over a period of 60 s. From the kinetic parameters reported by Al-Awadi *et al.*,[29] we may estimate an effective temperature of 700–750 K, considerably lower than that employed in other studies. The FTIR and GC results presented in Figs. 1 and 2, respectively, show that the major products arising from pyrolysis are 2-methylfuran (**5**), acetone and ketene (all in very similar amounts), the proportion of the first of these increasing slightly with laser power. The minor products observed were propadiene/propyne (C_3H_4 isomers), buta-1,3-diene, buta-1,2-diene, but-2-yne, methane and carbon monoxide. The observed production of acetone and ketene is in agreement with the study conducted by Hurd and Tallyn.[25] No short-lived products were detectable using matrix isolation spectroscopy, even using the shortest possible transit time between pyrolysis and matrix collection; co-pyrolysis with D_2 resulted in the production of a small amount of deuterated methane, but no other changes. The direct synthesis of **5** from acacH has not been previously reported; it is very likely that its formation in this work results from an H_2O elimination pathway similar to that proposed by Choudhury and Lin,[27] as discussed below.

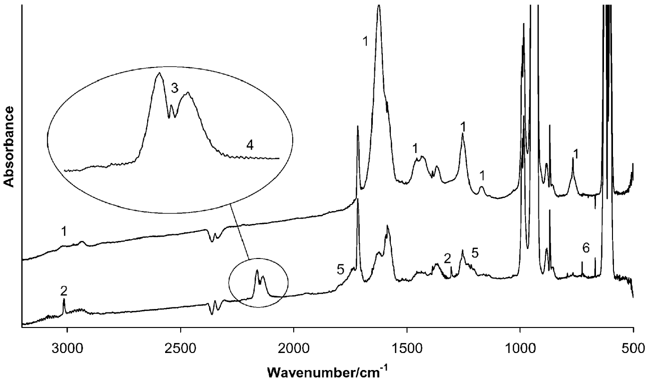

Fig. 1 Infrared spectra of acacH + SF_6 prior to (top) and following (bottom) IR LPHP. 1 = acacH, 2 = methane, 3 = ketene, 4 = CO, 5 = acetone, 6 = 2-methylfuran (**5**), unmarked = SF_6.

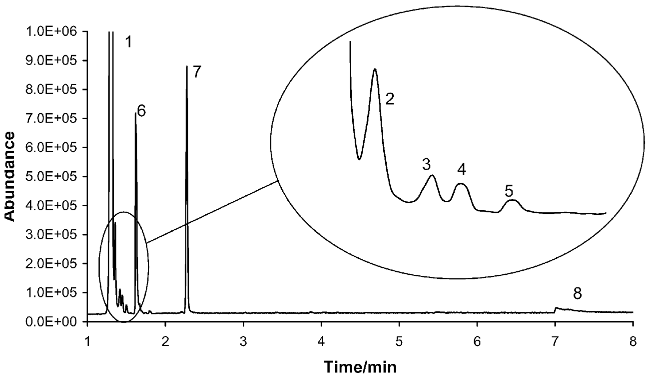

Fig. 2 GC trace of acacH + SF_6 following IR LPHP. 1 = SF_6, 2 = C_3H_4 (propadiene/propyne), 3 = buta-1,3-diene, 4 = buta-1,2-diene, 5 = but-2-yne, 6 = acetone, 7 = 2-methylfuran (**5**), 8 = acacH.

The results described above suggest that, under IR LPHP conditions, acacH undergoes decomposition *via* two concurrent pathways, one giving acetone and ketene, the other 2-methylfuran (**5**). As will be shown in the following discussion, the tautomeric nature of the β-diketone significantly influences the route of product formation. Evidently, the different structural configurations of the keto and enol tautomers yield quite distinct decomposition products.

Formation of acetone and ketene. Although acacH exists predominantly in the enol form (**1**), the keto (**4**) content does increase on raising the temperature, reaching *ca.* 40% at 230 °C.[24] Hence, the temperatures attained under IR LPHP conditions afford a sufficient amount of the acacH keto tautomer **4** to yield detectable pyrolysis products. Of the acacH tautomers, the keto form **4** bears the molecular structure most conducive to acetone formation. The decomposition of acacH to acetone and ketene was originally envisaged to proceed by a free radical mechanism, with α-β fission [reaction (1.1)] as the initiating step.[27] It is also conceivable that decomposition is initiated *via* β-γ bond fission [reaction (2.1)]; in either case, reaction is then envisaged to proceed by analogues of the Rice–Herzfeld mechanism for acetone,[31,32] as given in reactions (1.1)–(2.3):

$$CH_3COCH_2COCH_3 \rightarrow CH_3COCH_2^\bullet + {}^\bullet COCH_3 \qquad (1.1)$$

$$CH_3COCH_2^\bullet \rightarrow {}^\bullet CH_3 + CH_2{=}C{=}O \qquad (1.2)$$

$${}^\bullet CH_3 + {}^\bullet COCH_3 \rightarrow CH_3COCH_3 \qquad (1.3)$$

$$CH_3COCH_2COCH_3 \rightarrow CH_3COCH_2CO^\bullet + {}^\bullet CH_3 \qquad (2.1)$$

$$CH_3COCH_2CO^\bullet \rightarrow {}^\bullet CH_3CO + CH_2{=}C{=}O \qquad (2.2a)$$

$$CH_3COCH_2CO^\bullet \rightarrow {}^\bullet CH_3 + {}^\bullet COCH_2CO^\bullet \qquad (2.2b)$$

$${}^\bullet COCH_3 \rightarrow {}^\bullet CH_3 + CO \qquad (2.3)$$

To establish whether radical processes do indeed occur, co-pyrolysis studies of acacH with H_2 and D_2 (pressure: 2 torr) were conducted. Under these conditions, the radicals produced in the initial step [reaction (1.1)] above will be trapped with H_2 to produce acetone and acetaldehyde. Similarly, those of [reaction (2.1)] would yield methane and 3-oxobutanal (acetoacetaldehyde); the latter is known to be unstable, however, and self-condenses to form 1,3,5-triacetylbenzene.[33] In the presence of D_2, deuterated analogues of these products would be formed. The resultant FTIR and GC-MS analyses showed no indication of the formation of acetaldehyde or 3-oxobutanal, although acetone was produced. No evidence of deuterated acetone or acetaldehyde was found upon co-pyrolysis of acacH with D_2. While some deuteration of methane was detected, this is inconclusive, as it could well arise from the subsequent decomposition of acetone, a well-known radical process.[31,32]

An alternative six-centred unimolecular retroene mechanism[34] was proposed by Blades and Sandhu to account for the production of acetone from pyrolysis of acacH.[35] The activation energy (E_a) obtained from calculated Arrhenius *A* factors and experimentally determined rate constants was found to be 214 kJ mol^{-1}. This was revised downwards to 198.3 kJ mol^{-1} in the subsequent studies of Al-Awadi *et al.*[29]

In order to investigate these reactions further, we have performed calculations using PC Spartan '02 at the DFT/B3LYP/6-31G* level. The bond dissociation energies corresponding to reaction (1.1) and (2.1) were found to be 380 and 377 kJ mol^{-1}, respectively, whereas the activation energy *via* the retroene 6-centre transition state shown in Fig. 3 (left) was found to be 230 kJ mol^{-1}; no 4-centre transition state leading to ketene and acetone could be located. On the basis of the experimental evidence that free radicals are not involved, the much lower calculated activation energies for the molecular elimination route, and the good agreement with observed activation energies, we conclude that the formation of acetone and ketene is an intramolecular, rather than a free radical chain, process.

Formation of 2-methylfuran (5). Elimination of H_2O from acacH, as observed by Choudhury and Lin,[27] was suggested to occur *via* a four-centred transition state to produce pent-3-yn-2-one or penta-1,2-dien-4-one (acetylallene, **6**); the latter is illustrated in Fig. 3 (right). This elimination is readily facilitated when acacH adopts the enol form; its activation energy calculated at the DFT/B3LYP/6-311+G** level is 310 kJ mol^{-1}. The synthesis of acetylenic ketones from β-diketones is generally achieved by dehydrating with α,α-difluoroalkylamines.[36] **6** may be prepared from acacH by treating with triphenylphosphine dibromide to produce *E*/*Z*-2-bromo-4-oxo-2-pentene; dehydrobromination affords **6**.[37,38]

No direct evidence of either of these dehydration products was observed using FTIR or GC-MS. However, their involvement in the decomposition scheme of the enol form of acacH cannot be discounted, as both are known to rearrange readily. The pyrolytic rearrangement of pent-3-yn-2-ones (acetylenic ketones) has been shown to be an effective route towards the synthesis of cyclopentenones.[39] If pent-3-yn-2-one, the acetylenic ketone formed from dehydration of acacH, were to undergo such a reaction, cyclisation of the acetyl(methyl)vinylidene intermediate would produce 2-methylcyclobut-2-en-1-one. There is no evidence in the literature for preparation or isolation of the latter and no indication of its formation in this work.

On the other hand, the pyrolysis of allenyl ketones, such as **6** and hexa-1,2-dien-4-one, has been shown to lead to a rearrangement analogous to that of acetylenic ketones to produce furan derivatives. Huntsman and Yin[40] showed that synthesis of **5** was possible from the pyrolysis of **6**. Two possible mechanisms were offered to account for the formation of the rearrangement product, both involving a vinylidene intermediate and a 1,2-hydrogen shift and differing only in the sequence of these two processes; it was not clear which of these mechanisms is more likely. The significant aromatic stabilisation of furan may provide a sufficiently strong driving force to compete successfully with C–H insertion reactions in the carbenes.

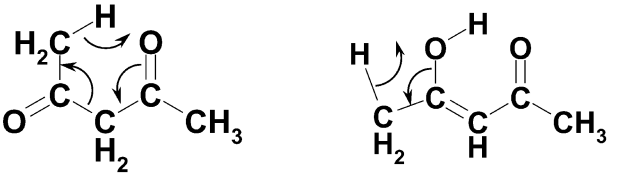

Fig. 3 Six-centred (left) and four-centred (right) transition states for the decomposition of acacH, leading to the formation of acetone + ketene and H_2O + penta-1,2-dien-4-one (**6**), respectively.

The work of Huntsman and Yin,[40] together with the pyrolysis study by Choudhury and Lin,[27] strongly suggest that IR LPHP of the enol form of acacH occurs initially with H_2O elimination to yield **6** as an intermediate, which readily rearranges to form **5**. Matrix isolation studies, which were performed in an effort to identify any intermediate or short-lived species, revealed no evidence of the pentadienone or any species other than unreacted acacH and ketene. There is no previous documentation of the synthesis of **5** from the direct decomposition of acacH and it therefore appears that a novel route to the production of **5** from IR LPHP of acacH has been established. Calculations at the DFT/B3LYP/6-31G* level showed that a simultaneous cyclisation and 1,2-hydrogen shift requires only 202 kJ mol^{-1}, confirming the very ready nature of this step under the prevailing conditions.

The minor products observed upon IR LPHP of acacH can be accounted for by the unimolecular decomposition of **5**, which produces a number of products including propadiene/propyne, buta-1,3-diene, buta-1,2-diene and but-2-yne. A reflected shockwave study by Liftshitz *et al.*[41] showed that the homogeneous unimolecular decomposition of **5** proceeds *via* 1,2-H atom migration from the C(5) to C(4) position. Stabilisation of the resultant intermediate is achieved by further 1,2-H atom migration and rearrangement to form CO, buta-1,3-diene, buta-1,2-diene and but-2-yne. Additionally, **5** may also undergo C–C bond cleavage after the initial 1,2-H atom migration process. This decomposition route yields C_3H_4 (propadiene/propyne) and ketene.

All observed products are thus accounted for and the corresponding routes are illustrated in Scheme 1.

1,1,1,5,5,5-Hexafluoropentane-2,4-dione (hexafluoroacetylacetone), hfacH (2)

Previous work. There has been little work reported on the thermal decomposition of **2**. There is, however, a substantial

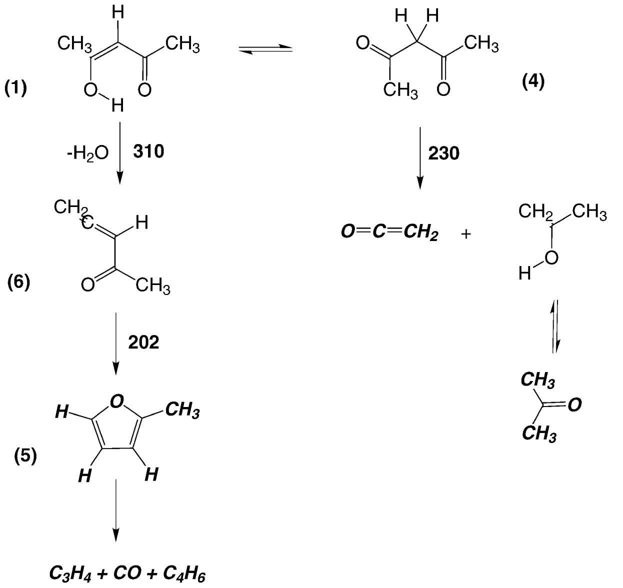

Scheme 1 Proposed reaction scheme for IR LPHP of acacH. Observed products in bold italics; numbers given are calculated activation energies in kJ mol^{-1}.

body of work on CVD related investigations of hfacH over metal and metal oxide surfaces,[42–48] while the photolysis study by Bassett and Whittle[49] is the only account of the homogeneous decomposition of **2**. Photolysis of the predominant enol form of **2** occurred with a novel HF elimination to yield 2,2-difluoro-5-(trifluoromethyl)furan-3(2*H*)-one (DHTF, **7**). Subsequent photolysis of this product produced CF_2 carbenes, which then inserted into the enolic OH bond of another hfacH molecule to produce 4-difluoromethoxy-1,1,1,5,5,5-hexafluoro-3-penten-2-one (DMHP, **8**). As part of a study on LaF_3 film formation from $La(hfac)_3 \cdot$diglyme, Condorelli *et al.*[50] investigated the thermal decomposition of **2** utilising a conventional hot-wall MOCVD system with a quartz reactor body; the heterogeneous formation of 1,1,1-trifluoroacetone and 1,1,1-trifluroacetaldehyde was observed.

Experimental results. Appreciable decomposition of **2** was effected upon IR LPHP at a laser power of approximately 6 W, corresponding to temperatures between 750 and 800 K. Fig. 4 presents FTIR spectra collected prior to and following pyrolysis; peaks attributable to carbon suboxide (C_3O_2), CF_2O, CO, $CF_2{=}CF_2$, CF_3H and SiF_4 were identified. SiF_4 arises from the reaction of HF with the Pyrex cell walls and it is therefore difficult to quantify fully the products in this system.

GC-MS analysis of heavier fragments (Fig. 5) detected unreacted **2**, trifluoroacetone (trace), C_3O_2 (16%), and three products with retention times of 1.43 (28%), 1.61 (32%) and 1.65 (23%) min. Analysis with the GasPro column aided in the detection of the lower molecular weight compounds $CF_2{=}CF_2$, CF_3H and CF_3CCH. The mass spectrum of the product eluted at 1.61 min was identical with the mass spectra obtained from the decomposition of a range of oxovanadium(IV) hfac complexes, $UO_2(hfac)_2$, and from UV photolysis of **2**.[49,51,52] This compound was identified as **7**. The mass spectrum of the compound eluted at 1.65 min was attributed, upon comparison with mass spectral data obtained by Bassett and Whittle, to **8**, that is, the product resulting from CF_2 carbene insertion into the O–H bond of a hfacH molecule following UV photolysis.[49] The product eluted at 1.43 min has not been previously observed. Its mass spectrum (Fig. 6) exhibits a parent mass fragment at m/z = 110. No product possessing such a mass spectrum has been reported from previous decomposition studies of **2** or complexes containing **2**. FTIR spectra provided no indication of the identity of this product. However, a very likely candidate on the basis of the mass spectra of similar compounds is 3,3-difluoroacryloylfluoride, $CF_2{=}CH{-}CFO$ (DFAF, **9**). For example, the mass spectrum of benzoyl fluoride, C_6H_5COF, exhibits strong peaks at m/z = 124 (M), 105 (M − 19), 86 (M − 28), and 77 (M − 47), a pattern also evident in Fig. 6.[53]

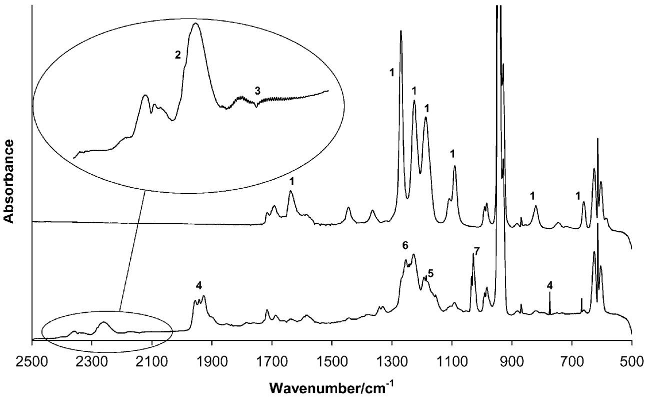

Fig. 4 Infrared spectra of **2** + SF_6 prior to (top) and following (bottom) IR LPHP. 1 = hfacH (**2**), 2 = carbon suboxide, 3 = CO, 4 = carbonyl fluoride, 5 = trifluoromethane, 6 = tetrafluoroethene, 7 = SiF_4, unmarked = SF_6.

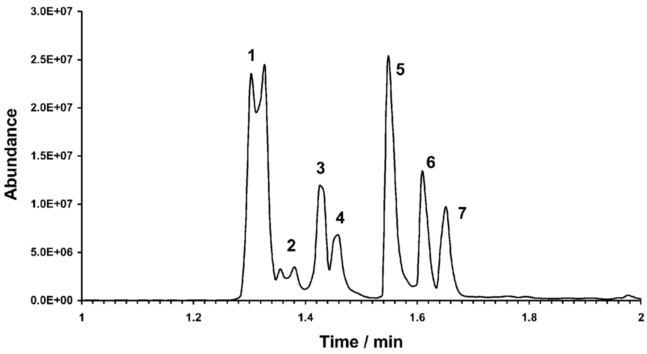

Fig. 5 GC trace of **2** + SF_6 following IR LPHP. 1 = SF_6, 2 = trifluoroacetone, 3 = DFAF (**9**), 4 = carbon suboxide, 5 = hfacH (**2**), 6 = DHTF (**7**), 7 = DMHP (**8**).

Co-pyrolysis with H_2 or D_2 (2 torr) did not result in incorporation of D into any products or the generation of new products, suggesting that free radicals are not involved. Matrix isolation studies did reveal a number of bands of species in the 2100 to 2300 cm^{-1} region (characteristic of cumulative double bonds or triple bonds), as shown in Fig. 7. Although the spectra are complex and overlapped, and assignment is far from certain, a band identified as arising from a transient species at 2194 cm^{-1} is consistent with the gas-phase harmonic value of 2252 cm^{-1} calculated for trifluoromethylketene, adjusted by the usual corrections for anharmonicity and matrix effects.[54]

Formation of 2,2-difluoro-5-(trifluoromethyl)furan-3(2*H*)-one (DHTF, 7) and 4-difluoromethoxy-1,1,1,5,5,5-hexafluoro-3-penten-2-one (DMHP, 8). The results obtained indicate that the primary decomposition products of **2** are C_3O_2, **7**, **9** and **8** (and, by implication, HF); the minor products COF_2, C_2F_4, CF_3H, trifluoromethylacetylene and trifluoroacetone arise, as discussed below, from subsequent decomposition of the primary products. The most likely route identified by calculation was indeed the HF molecular elimination route, with an activation energy calculated at 196 kJ mol^{-1}, thus accounting for the formation of **7** and SiF_4. **8** arises from insertion of a CF_2 carbene into the O–H bond of the enol form of **2**; the most likely origin of the CF_2 is DHTF itself, as observed by Bassett and Whittle in their photolysis study.[49] CF_2 may also dimerise, of course, yielding the observed tetrafluoroethene. All these products and formation routes are illustrated in Scheme 2.

Formation of 3,3-difluoroacryloylfluoride and carbon suboxide. No dehydration routes analogous to acacH are possible. Instead, the most likely secondary (higher temperature) pathway involves semi-concerted loss of CF_3 radicals, followed by

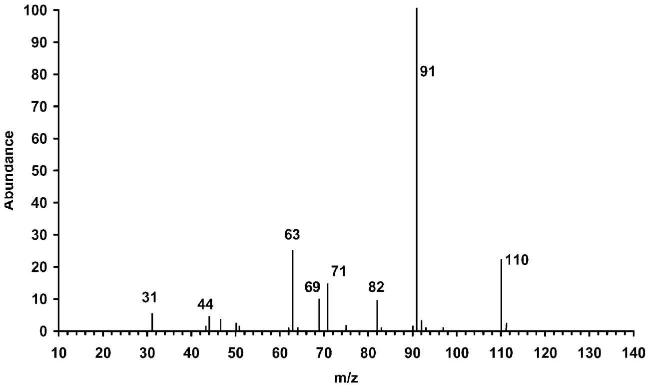

Fig. 6 Mass spectrum of the product of IR LPHP of **2** eluted with a retention time of 1.43 min, ascribed to DFAF (**9**).

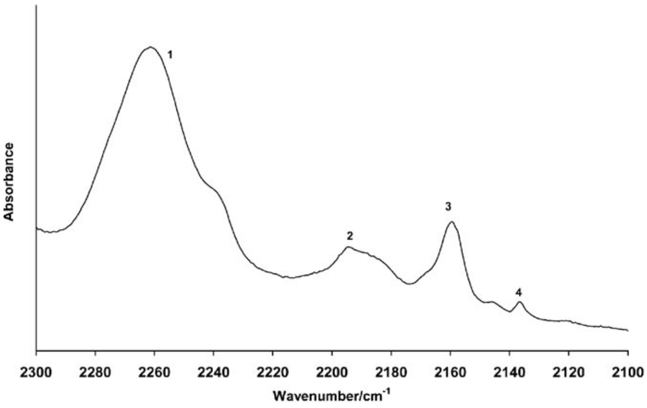

Fig. 7 Partial FTIR spectrum of matrix isolated products of IR LPHP of **2** + SF_6. Peaks 1, 3 and 4 are not affected by mild annealing and are assigned to carbon suboxide, trifluoromethylacetylene and CO, respectively; peak 2 disappears on annealing and is assigned to an unstable ketene (see text).

abstraction of the labile central H from the parent hfacH to give the observed CF_3H. This pathway has an activation energy of approximately 290 to 300 kJ mol^{-1}, based on our calculations and the reported CF_3–C bond strength in CF_3COCH_3.[55] Loss of one CF_3H results in trifluoroacetylketene (**10**) and loss of a second CF_3H yields the observed relatively stable C_3O_2. **10** is unstable and has not been isolated to date; it is therefore likely to undergo further reaction in the IR LPHP system. By analogy with well-known pyrolytic pathways in ketenes, a possible sequence of events is: (i) decarbonylation—an activation energy in the typical range of 200–240 kJ mol^{-1} would allow this reaction to proceed very rapidly, resulting in the carbene **11**;[56] (ii) the familiar Wolff rearrangement (activation energies typically 10–50 kJ mol^{-1}) of the resultant trifluoroacetylcarbene **11** to yield trifluoromethylketene (**12**);[57,58] (iii) a 1,3-F shift resulting in **9**. This last step is somewhat unexpected at first sight, since 1,3-shifts are generally assumed to be thermally forbidden, but our calculations at the DFT/B3LYP/6-31G* level predict an activation energy of just 180 kJ mol^{-1} for this step. This migratory ease has also been demonstrated in a study of 1,3-sigmatropic shifts in carbonylketenes and similar compounds.[59] Thus, each step in this sequence is quite feasible under the prevailing conditions; the matrix isolation detection of a vibration characteristic of ketenes at 2194 cm^{-1} lends additional weight to this hypothesis.

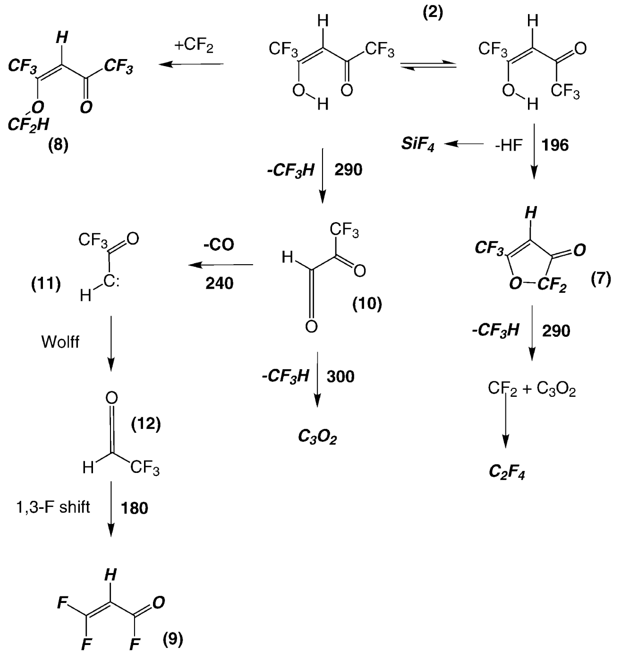

Scheme 2 Proposed reaction scheme for IR LPHP of **2**. Observed products in bold italics; numbers given are calculated activation energies in kJ mol^{-1}.

2,2,6,6-Tetramethylheptane-3,5-dione, thdH (3)

Previous work. The thermal decomposition of **3** under MOCVD conditions has been studied by a number of workers, largely to complement decomposition studies of the corresponding metal complexes. Condorelli *et al.*[60] investigated the thermal decomposition of **3** under MOCVD conditions as part of a study of the decomposition of $Cu(thd)_2$. Their observations suggested the presence of two different reaction paths depending on temperature. Decomposition was observed to commence at temperatures above 400 °C with cleavage of the αC–βCO bond to afford 3,3-dimethylbutan-2-one (**13**). The remaining C_5H_8O moiety was proposed to rearrange to form a cyclic ether (3-methyl-2,5-dihydrofuran), the rationale being that the observed ν(CO) at 1075 cm^{-1} was more consistent with that of furan rather than an aliphatic ether. In the high temperature route (500–600 °C), Condorelli *et al.* suggested that the initial stage of thdH decomposition involved dehydration to form $(CH_3)_3CCOCHC_5H_8$, which subsequently decomposed to yield 3-methylpenta-1,4-diene, methylketene and ethene.

The elimination of H_2O as the initial step of decomposition was also proposed by Bykov *et al.*[61] in their mass spectrometric study of the thermolysis of **3**. Decomposition occurred at approximately 590 °C and, analogous to the work of Condorelli *et al.*,[60] dehydration resulted in the production of a $(CH_3)_3CCOCHC_5H_8$ moiety, which eliminated methyl and ethyl radicals with increased temperature. Their observations also indicated that the thermal stability of **3** was lowered significantly in the presence of oxygen.

The lower temperature decomposition route observed by Condorelli *et al.* is also supported by similar results by other workers. A GC-MS study by Lopaeva *et al.*[62] found that the gas phase decomposition of **3** at 400 °C produced **13**, isobutene (2-methylpropene, **14**) and carbon monoxide. The formation of 3,3-dimethyl-2-butanone along with 2,2-dimethylpropanal and **14** was also observed upon decomposition of **3** at 484 °C by Obi-Johnson.[63]

In summary, literature reports suggest that the decomposition of **3** proceeds by two different pathways influenced by temperature. Dehydration occurs at higher temperature (600 °C) while at lower temperature (400–484 °C) αC–βCO bond scission is effected.

Experimental results. Appreciable decomposition of **3** was effected upon pyrolysis at a laser power of approximately 6 W (700–750 K). The sole significant decomposition product of **3** detectable using GC-MS was isobutene (**14**); other products observed in trace amounts included 2-methylbuta-1,3-diene (isoprene), 2-methylbut-1-ene and but-1-en-3-yne. Use of the GasPro column aided in the detection of **14**, propene, 2-methylpropane (isobutane) and trace amounts of propadiene, 1-butyne, methane and propyne. Because of the low vapour pressure of **3**, pressures were limited to 0.25 torr. Although sufficient to permit IR LPHP, such a low reagent pressure produces weak infrared spectra, which can hinder the monitoring of reaction progress and the identification of products. However, the FTIR spectrum obtained following pyrolysis of **3** did reveal peaks attributable to unreacted **3**, ketene and CO, as shown in Fig. 8. No bands due to **14** or isobutane were detectable by FTIR.

These results at first sight suggest that the decomposition of **3** occurs *via* a mechanism that involves the production of

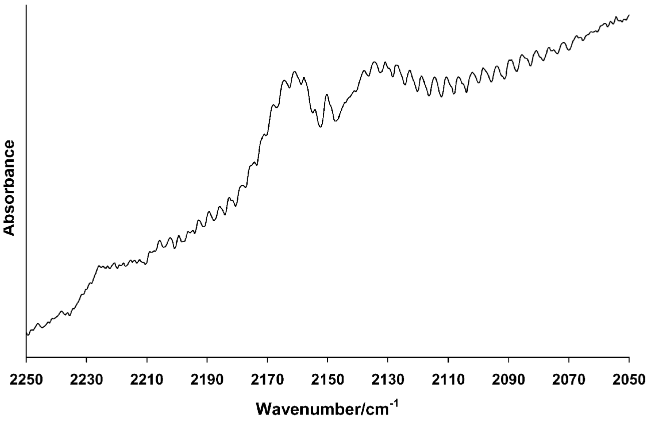

Fig. 8 Partial FTIR spectrum of products of IR LPHP of **3**, confirming the formation of ketene and CO (compare insert of Fig. 1).

t-butyl radicals; disproportionation of *t*-butyl radicals affords isobutane and **14**. A second possible reaction route involves homolysis to produce other radicals and subsequent loss of carbon monoxide and ketene. Supplementary pyrolysis studies were therefore conducted to investigate the involvement of *t*-butyl radicals and provide further insight into the decomposition of **3**.

Co-pyrolysis studies of **3** with H_2 were undertaken in an effort to confirm the formation and involvement of *t*-butyl radicals. If *t*-butyl radicals are indeed produced, then reaction with H_2 should compete with disproportionation to facilitate formation of isobutane. Hence, an increase in isobutane production would be observed. In practice, the co-pyrolysis of **3** with H_2 did not significantly affect the product distribution of **14** and isobutane. However, two additional products not previously observed in the pyrolysis of **3** alone were detected in significant amounts by GC-MS. These two compounds were eluted with retention times of 3.12 (trace) and 4.13 min, and were identified as 3-methylbutan-2-one (**15**) and **13**, respectively. The formation of these products would require that the first step involve homolysis of the bond between the α-carbon and β-carbonyl. Subsequent reaction of the resulting radical species with H_2 would then yield 3,3-dimethylbutan-2-one and 2,2-dimethylpropanal (pivalaldehyde, **16**). No evidence of 2,2-dimethylpropanal was found, but the ready isomerisation of this compound does produce the observed **15**.[64] In the presence of D_2, there was clear evidence of incorporation of a single D atom into these products. On the other hand, matrix isolation studies did reveal features consistent with *t*-butyl radicals when the shortest transfer time was used. Partially overlapped peaks observed at 2942 (2936), 2825 (2825) and 1456 (1455) cm^{-1} disappeared on annealing (reported values in parentheses, the reported peak at 1366 cm^{-1} being completely obscured by the parent thdH[65,66]), and radicals are evidently formed at some stage during the pyrolysis.

Discussion. α-Carbon–β-carbonyl bond homolysis of the enol form will produce the radicals shown in Scheme 3. Each radical then loses either CO or ketene to yield *t*-butyl radicals; these processes are likely to proceed very rapidly, their calculated activation energies being 110 and 190 kJ mol^{-1}, respectively. On the other hand, trapping with hydrogen will produce 3-dimethyl-1-buten-2-ol, which is essentially the enol tautomer of 3,3-dimethylbutan-2-one, and **16**, a well-known precursor to **15**.[64] 3,3-Dimethylbutan-2-one is significantly more stable than its enol tautomer; its enol-keto equilibrium constant pK_E[67] of 8.33 [68] is comparable to that of acetone (8.76).[69]

Obi-Johnson[63] found that **3** decomposed to produce 3,3-dimethyl-2-butanone and 2,2-dimethylpropanal, with no addition of a hydrogen source. This particular study, however, was conducted under MOCVD conditions, so it is likely that heterogeneous reactions with hydrogen-containing species on the reactor surface lead to the formation of these products. The absence of 2,2-dimethylpropanal (or its isomer, 3-methyl-2-butanone) in the work of Lopaeva *et al.*[62] led these authors to suggest a unimolecular decomposition route involving intramolecular hydrogen atom transfer to yield 3,3-dimethylbutan-2-one, CO and **14**. Although the reaction conditions utilised by both workers did not differ significantly, the difference in the GC-MS columns used in the studies by Obi-Johnson and Lopaeva *et al.* may account for the disparity in the products observed.

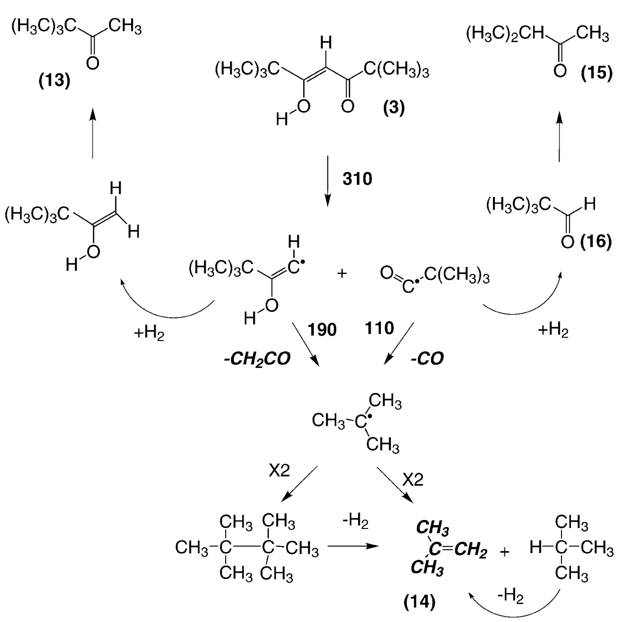

Scheme 3 Proposed reaction scheme for IR LPHP of **3**. Observed products in bold italics; numbers given are calculated activation energies in kJ mol^{-1}. Also shown is the formation of products on trapping initial radicals with H_2.

The formation of mono-deuterated 3,3-dimethylbutan-2-one upon co-pyrolysis of **3** with D_2 in this work provided evidence of αC–βCO bond scission and thus precluded the involvement of an intramolecular mechanism. The corresponding aldehyde was not observed, but as mentioned previously, 2,2-dimethylpropanal is capable of isomerising to **15**. Traces of the latter were detected, in its mono-deuterated form, on co-pyrolysis with D_2.

The initially proposed route to thdH decomposition involving homolysis to produce *t*-butyl radicals as the first step must therefore be reconsidered in light of the co-pyrolysis results. The IR LPHP of **3** instead appears to be consistent with a mechanism involving firstly homolysis of the αC–βCO bond to produce $(CH_3)_3CC({=}O)^\bullet$ and $(CH_3)_3CC(OH){=}CH^\bullet$ radicals. As observed from co-pyrolysis studies, the addition of hydrogen to these radicals produces 3,3-dimethyl-2-butanone and 3-methyl-2-butanone, respectively. In the absence of hydrogen, it is proposed that the radicals $(CH_3)_3CC({=}O)^\bullet$ and $(CH_3)_3CC(OH){=}CH^\bullet$ undergo very ready further homolysis to produce *t*-butyl radicals and CO or ketene, as shown in Scheme 3. A slight preference for this α,β homolysis is confirmed by calculation of the bond energies. Loss of a *t*-butyl radical requires 328 kJ mol^{-1}, whereas loss of $(CH_3)_3C$–CO requires 310 kJ mol^{-1}, a difference leading to a ratio in the rates of approximately 40 at the pyrolysis temperature. No competitive molecular routes were revealed by calculation, in accord with the radical routes revealed by the co-pyrolysis studies. All observed major products are accounted for in Scheme 3; trace products may be ascribed to partial further decomposition of the principal products.

Conclusions

The three β-diketones investigated here show very different decomposition pathways. Where feasible, low-energy molecular elimination mechanisms, such as the production of ketene and acetone or dehydration in acacH, or the loss of HF from **2**, dominate; of course, the primary products of such pathways may themselves be subject to further reaction and therefore not directly observable. In other cases, where no low-energy molecular route is available, radical pathways are significant. In each case, calculations of the proposed pathways support the experimental observations and deductions.

Of course, the proposed pathways will have a profound effect on the chemistry of decomposition of metal complexes. For example, the production of HF will almost certainly lead to the formation of metal fluorides, as has been observed using many hfac complexes.[64] These factors will be explored in our future work.[15]

Acknowledgements

We thank the University of Auckland for assistance with the purchase of equipment, and the Department of Chemistry for a doctoral scholarship to AY.

References

1 R. C. Mehrotra, R. Bohra and D. P. Gaur, *Metal β-Diketonates and Allied Derivatives*, Academic Press, London and New York, 1978.

2 (*a*) G. B. Stringfellow, *Organometallic Vapor Phase Epitaxy: Theory and Practice*, Academic Press, Boston, 1989; (*b*) *The Chemistry of Metal CVD*, eds. T. T. Kodas and M. J. Hampden-Smith, Weinheim, New York, 1994.

3 J. M. Shaub and S. H. Bauer, *Int. J. Chem. Kinet.*, 1975, **7**, 509.

4 J. Pola, *Collect. Czech. Chem. Commun.*, 1981, **46**, 2856.

5 G. A. Atiya, A. S. Grady, S. A. Jackson, N. Parker and D. K. Russell, *J. Organomet. Chem.*, 1989, **260**, 180.

6 D. K. Russell, *Chem. Soc. Rev.*, 1990, **19**, 407.

7 D. K. Russell, I. M. T. Davidson, A. M. Ellis, G. P. Mills, M. Pennington, I. M. Povey, J. B. Raynor, S. Saydam and A. D. Workman, *Organometallics*, 1995, **14**, 3717.

8 D. K. Russell, *Adv. Mater. CVD*, 1997, **2**, 223.

9 R. A. Berrigan, J. B. Metson and D. K. Russell, *Adv. Mater. CVD*, 1998, **4**, 23.

10 J. E. Everett, N. D. Renner and D. K. Russell, *Chem. Commun.*, 1998, 341.

11 I. M. T. Davidson, A. M. Ellis, G. P. Mills, M. Pennington, I. M. Povey, J. B. Raynor, D. K. Russell, S. Saydam and A. D. Workman, *Adv. Mater. CVD*, 1998, **4**, 103.

12 N. R. Hore and D. K. Russell, *J. Chem. Soc., Perkin Trans. 2*, 1998, 269.

13 N. R. Hore and D. K. Russell, *New J. Chem.*, 2004, **28**, 606.

14 H. Hettema, N. R. Hore, N. D. Renner and D. K. Russell, *Aust. J. Chem.*, 1998, **50**, 363.

15 D. K. Russell and A. Yee, in preparation.

16 J. L. Lyman, *J. Chem. Phys.*, 1977, **67**, 1868.

17 S. Davison and M. Barton, *J. Am. Chem. Soc.*, 1952, **74**, 2307.

18 G. H. Miller and E. W. R. Steacie, *J. Am. Chem. Soc.*, 1958, **80**, 6486.

19 R. R. Baldwin, R. W. Walker and D. H. Langford, *Trans. Faraday Soc.*, 1969, **65**, 2116.

20 *PC Spartan '02*, Wavefunction, Inc.,, Irvine, CA, 2001.

21 *Spartan '02 Tutorial and User's Guide*, Wavefunction, Inc., Irvine, CA, 2001.

22 J. J. P. Stewart, *J. Comput. Aided Mol. Des.*, 1990, **4**, 1.

23 N. I. Butkovskaya, Y. Zhao and D. W. Setser, *J. Phys. Chem. A*, 1994, **98**, 10779.

24 E. Funcke and R. Mecke, in *Hydrogen Bonding*, ed. D. Hadzi, Pergamon Press, London, 1959, p. 433.

25 C. D. Hurd and W. H. Tallyn, *J. Am. Chem. Soc.*, 1925, **47**, 1779.

26 R. G. Charles, W. M. Hickam and J. von Hoene, *J. Phys. Chem.*, 1959, **63**, 2084.

27 T. K. Choudhury and M. C. Lin, *Int. J. Chem. Kinet.*, 1990, **20**, 491.

28 For consistency among the three systems, we have adopted the common convention of lettering the central C atom in the –CO–CH_2–CO- unit as α, so that the carbonyl C is β, *etc.*

29 N. A. Al-Awadi, M. H. El-Nagdi and T. Mathew, *Int. J. Chem. Kinet.*, 1995, **27**, 517.

30 N. A. Al-Awadi, M. H. El-Nagdi, H. A. Al-Awadhi and O. M. E. El-Dusouqui, *Int. J. Chem. Kinet.*, 1998, **30**, 457.

31 F. O. Rice and K. F. Herzfeld, *J. Am. Chem. Soc.*, 1934, **56**, 284.

32 S. H. Mousavipour and P. D. Pacey, *J. Phys. Chem.*, 1996, **100**, 3573.

33 R. Kaushal, S. Sovani and S. S. Deshapande, *J. Indian Chem. Soc.*, 1942, **19**, 107.

34 D. V. Banthorpe, *Elimination Reactions*, Elsevier, Amsterdam, 1963.

35 A. T. Blades and H. S. Sandhu, *Int. J. Chem. Kinet.*, 1971, **3**, 187.

36 T. Kitazume and N. Ishikawa, *Chem. Lett.*, 1980, 1327.

37 T. Constantieux and G. Buono, *Org. Synth.*, 2000, **78**, 135.

38 G. Buono, *Synthesis*, 1981, **11**, 872.

39 M. Karpf and A. S. Dreiding, *Helv. Chim. Acta*, 1979, **62**, 852.

40 W. D. Huntsman and T. K. Yin, *J. Org. Chem.*, 1983, **48**, 3813.

41 A. Lifshitz, C. Tamburu and R. Shashua, *J. Phys. Chem. A*, 1997, **101**, 1018.

42 S. R. Droes, T. T. Kodas and M. J. Hampden-Smith, *Adv. Mater.*, 1998, **10**, 1129.

43 M. A. George, D. W. Hess, S. E. Beck, J. C. Ivankovits, D. A. Bohling and A. P. Lane, *J. Electrochem. Soc.*, 1995, **142**, 961.

44 S. W. Kang, H. U. Kim and S. W. Rhee, *J. Vac. Sci. Technol., B*, 1999, **17**, 154.

45 H. L. Nigg and R. I. Masel, *Surf. Sci.*, 1998, **409**, 428.

46 H. L. Nigg and R. I. Masel, *J. Vac. Sci. Technol., A*, 1999, **17**, 3477.

47 J. E. Parmeter, *J. Phys. Chem.*, 1993, **97**, 11530.

48 F. Rousseau, A. Jain, T. T. Kodas, M. Hampden-Smith, J. D. Farr and R. Muenchausen, *J. Mater. Chem.*, 1992, **2**, 893.

49 J. E. Bassett and E. Whittle, *Int. J. Chem. Kinet.*, 1976, **8**, 859.

50 G. G. Condorelli, S. Gennaro and L. Fragala, *Chem. Vap. Deposition*, 2000, **6**, 185.

51 D. A. Johnson and A. B. Waugh, *Polyhedron*, 1983, **2**, 1323.

52 A. Ekstrom, H. Hurst and C. H. Randall, *J. Phys. Chem.*, 1982, **86**, 2375.

53 *"Mass Spectra", NIST Chemistry WebBook, NIST Standard Reference Database no 69*, eds. P. J. Linstrom and W. G. Mallard, NIST Mass Spec. Data Center (Director: S. E. Stein), Gaithersburg, MD, March 2003.

54 W. Förner, H. M. Badawi, A. A. Al-Saadi and S. A. Ali, *J. Mol. Model.*, 2001, **7**, 343.

55 *Handbook of Chemistry and Physics*, ed. R. C. Weast, 60th edn., CRC Press, Boca Raton, FL, 1980.

56 K. M. Forsythe, S. K. Gray, S. J. Klippenstein and G. E. Hall, *J. Chem. Phys.*, 2001, **115**, 2134.

57 L. Wolff, *J. Liebigs Ann. Chem.*, 1902, **325**, 129.

58 W. Kirmse, *Eur. J. Org. Chem.*, 2002, 2193.

59 M. T. Nguyen, L. Landuyt and H. M. T. Nguyen, *Eur. J. Org. Chem.*, 1999, 401.

60 G. G. Condorelli, M. L. Hitchman, A. Y. Kovalgin and S. H. Shamlian, *Proc. Electrochem. Soc.*, 1999, **98-23**, 141.

61 A. F. Bykov, P. P. Semyannikov and I. K. Igumenov, *J. Therm. Anal.*, 1992, **38**, 1463.

62 O. V. Lopaeva, M. L. Hitchman, S. H. Shamlian and D. R. Watson, *J. Phys. IV: Proceedings 12 (13th Eur. Conf. on CVD, 2001)*, 2002, **12**, Pr4/85.

63 B. J. Obi-Johnson, *PhD Thesis*, Georgia Institute of Technology, Atlanta, GA, 1999 (*Chem. Abs.*, 2000, **133**, 114055; *Diss. Abs. Int.*, 2000, **60**, 3255).

64 S. M. Fine, P. N. Dyer, J. A. T. Norman, B. A. Murator and R. L. Iampietro, *Mater. Res. Soc. Symp. Proc.*, 1990, **204**, 415 (*Chem. Abs.*, 1990, **115**, 244964).

65 J. Pacansky and J. S. Chang, *J. Chem. Phys.*, 1981, **74**, 5539.

66 B. Schrader, J. Pacansky and U. Pfeiffer, *J. Chem. Phys.*, 1984, **88**, 4069.

67 In aqueous solution at 25 °C.

68 J. R. Keefe, A. J. Kresge and N. P. Schnepp, *J. Am. Chem. Soc.*, 1990, **112**, 4862.

69 Y. Chiang, A. J. Kresge and N. P. Schnepp, *J. Am. Chem. Soc.*, 1989, **111**, 9677.